

Enhancing the Radiation Pattern of Phase Array Antenna Using Particle Swarm Optimization

¹J.J. Biebuma, ²B. O. Omijeh, ³E. L. Jackson

^{1,2,3} Department of Electronic & Computer Engineering University of Port Harcourt, Rivers State, Nigeria.

Abstract: Phase array antenna radiates a signal pattern whose side lobes compared to the main lobe is higher than the acceptable value and become more pronounced when the array is steerable (scanning array). Despite efforts made by array designers to control this defect, have still not solved the problem of power losses in undesired directions and radio signal interference with other frequency signals. In this paper, a modified particle swarm optimization program has been proposed. The program finds the values of current excitation that will minimize sidelobe level and achieve a radiation pattern that matches closely with the desired pattern. The Particle Swarm Optimization program forms a part of a 24 array antenna model, and the whole idea is simulated in MATLAB environment. Results obtained are very satisfactory. When fully implemented by array designers, power losses will greatly reduce and radio link communication will greatly improve.

Keywords: Radiation, Antenna, Optimization, Swarm, Matlab

I. Introduction

One of the setbacks of phase array antenna is power losses due to high sidelobes in its radiation pattern. Sidelobes map out the portion of the transmitted power that is wasted in undesired direction. Several authors have carried out research studies on array pattern optimization. Linear antenna array was optimized using genetic algorithm for reduction in side lobe levels and directivity improvement (Pallavi, 2013). In his paper, Genetic algorithm Solver in Optimization toolbox of MATLAB was used to obtain maximum reduction in side lobe level relative to the main beam on both sides of 0° to improve the directivity. Genetic algorithm is an intellectual algorithm that searches for the optimum element weight of the array antenna. His paper demonstrated the different ways to apply Genetic algorithm by varying number of elements to optimize the array pattern. Adaptive feasible mutation with single point crossover showed the performance improvement by reducing the side lobe level below -10dB in most of the cases and also improved the directivity. The best result of -21.05dB sidelobe is obtained for 20 elements in 50 generation of GA with best fitness value of 27.2451 and mean fitness value of 27.3439 and improved the directivity to 16.96^0 level. The best result of 17.98^0 directivity was obtained for 24 elements.

When antennas elements are arrayed in a certain geometrical configuration, the signal induced on them are combined to form the array output. A plot of the array response as a function of angle is normally referred to as the array pattern or beam pattern. Synthesizing the array pattern of antenna array has been a subject of several studies and investigations. The trade-off between the side-lobe levels (SLL) and the half-power beamwidth (HPBW) stimulate the question answered primarily by Dolph of obtaining the narrowest possible beamwidth for a given side-lobe level or the smallest side-lobe level for a given beamwidth (Haupt, 1986). This was possible by using the orthogonal functions of Chebyshev in order to design an optimum radiation pattern (Drabowitch, etal 1998). However, for large number of elements this procedure becomes quite cumbersome since it requires matching the array factor expression with an appropriate Chebyshev function (Balanis, 2005). To overcome this deficiency, Safaai-Jazi proposed a new formulation for the design of Chebyshev arrays based on solving a system of linear equations (Safaai-Jazi, 1994). The forgoing mentioned investigations either require analytical formulae or evaluating the gradient of some objective function, which sometimes become formidable to evaluate. As alternatives, neural network and evolutionary algorithms techniques were used in order to reduce the side lobes of linear arrays (Dahab, etal 1998). Genetic algorithms (GA) and particle swarm optimization are well-known evolutionary algorithm techniques (Rahmat-Samii, etal 1999). In GA, a sample of possible solutions is assumed then mutation, crossover, and selection are employed based on the concept of survival of the fittest. On the other hand, PSO is a much easier algorithm in which each possible solution is represented as a particle in the swarm with a certain position and velocity vector. The position and velocity of each particle are updated according to some fitness function. Some studies have been devoted to compare between the GA and PSO and a general conclusion has been reached that the PSO shows better performance due to its greater implementation simplicity and minor computational time.

Since it has been introduced by Kennedy and Eberhard, the PSO is being applied to many fields of endeavor.

Surprisingly, it has been applied to the design of low dispersion fiber Bragg gratings (Basker, etal, 2005), and to the design of corrugated horn antenna.

Phased arrays operate using an electrically or mechanically steered beam. Multiple antenna elements are used, but their transmitted (or received) signals are phase shifted so as to alter the direction of the antenna's broadcast. This apparent steering is caused by constructive interference in the direction of interest and destructive interference in directions of no interest (Balanis, 2005). The phase shifting can be done by analog or digital phase shifters. With the analog method, varactor diodes, whose reactance can be changed by a bias voltage, are used to control phase. In the digital domain, there are a variety of digital phase shifter chips that are used (<http://www.microwaves101.com/encyclopedia/phaseshifters.cfm>).

II. Theoretical Background Of Phased Array Antennas

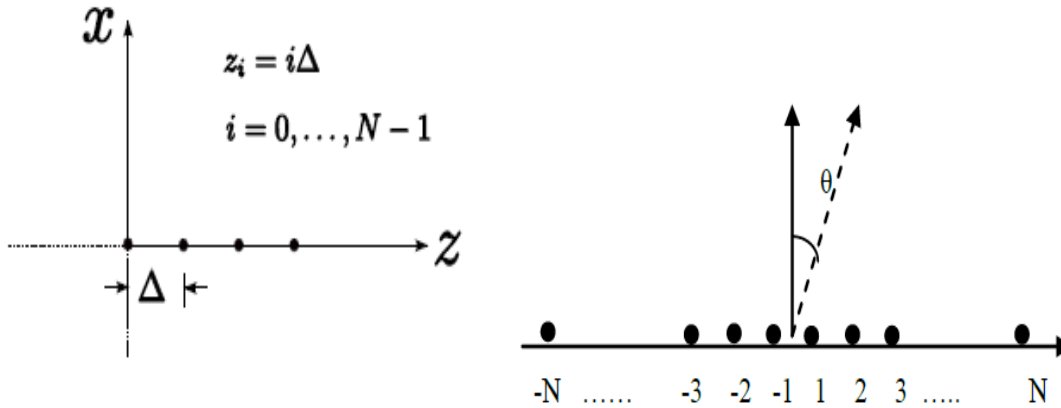


Fig 1.1 Uniform linear array of N element along the z-axis **Fig 3.1** Geometry of array element of size 2N

A uniform linear array antenna is one whose elements have equal amplitude and are spaced equally along one dimension. In figure 1.1, maximum beam occurs for $\theta_0 = 90^\circ$. If we center array about $z=0$, and normalize, the array factor will become

$$|E_a(\theta)| = \frac{1}{\sqrt{N}} \left| \frac{\sin(N2\pi/\lambda(d \sin \theta/2))}{\sin(2\pi/\lambda(d \sin \theta/2))} \right| \dots\dots\dots (2.1)$$

The radiation pattern of a phase array antenna is

Radiation pattern = Element pattern × array factor

For isotropic sources, the radiation pattern is equal to the array factor.

III. Design Methodology

3.1 Modeling of antenna pattern

The electric field of a linear array of isotropic sources is given by

$$E_a(\theta) = 1/\sqrt{N}(I) \sum_{n=1}^N e^{-j2\pi\lambda(nd \sin \theta_0 - \theta_s)} \quad (\text{simon, etal, 2007}) \dots\dots\dots (3.2)$$

Where $E_a(\theta)$ = electric field at angle θ , n = element number, d = inter-element spacing, Φ_n = phase shift per element, θ_s = scan angle, θ_0 = broadside I = current excitation, λ = wavelength

For a uniformly excited array, $I = 1$.

Rewriting eqn 3.2 in series expansion form

$$E_a(\theta) = I(1 + e^{j2\pi\lambda(nd \sin \theta)} + \dots\dots\dots + e^{(N-1)j2\pi\lambda(nd \sin \theta)}) \dots\dots\dots (3.3)$$

This is a geometric series and can be expressed as

$$E_a(\theta) = \frac{1 - e^{-j2\pi\lambda(nd \sin \theta)}}{1 - e^{-j2\pi\lambda(nd \sin \theta)}}; \quad \text{The far field array intensity pattern is given by}$$

$$|E_a(\theta)| = \sqrt{E(\theta)E^*(\theta)} \quad \dots\dots\dots (3.4)$$

substitution gives

$$|E_a(\theta)| = \sqrt{\frac{(1 - \cos N2\pi/\lambda(d \sin \theta))^2 + (\sin N2\pi/\lambda(d \sin \theta))^2}{(1 - \cos 2\pi/\lambda(d \sin \theta))^2 + (\sin 2\pi/\lambda(d \sin \theta))^2}}$$

But $1 - \cos \theta = 2(\sin \theta / 2)$

therefore , $|E_a(\theta)| = \left| \frac{\sin(N2\pi/\lambda(d \sin \theta/2))}{\sin(2\pi/\lambda(d \sin \theta/2))} \right| \dots\dots\dots (3.5)$

The maximum value occurs at $\theta_0 = 90$ and is N. therefore normalizing gives

$|E_a(\theta)| = \frac{1}{\sqrt{N}} \left| \frac{\sin(N2\pi/\lambda(d \sin \theta/2))}{\sin(2\pi/\lambda(d \sin \theta/2))} \right| \dots\dots\dots (3.6)$

And the Gain of the beam pattern is

$|G_a(\theta)| = |E_a(\theta)|^2 = \frac{1}{N} \left| \frac{\sin(N2\pi/\lambda(d \sin \theta/2))}{\sin(2\pi/\lambda(d \sin \theta/2))} \right|^2 \dots\dots\dots (3.7)$

As N tends to infinity this becomes a sinc function.

Equation (3.7) is the derived Gain for a linear phase array isotropic antenna of N- elements. In this paper, the gain of the array of 4, 8, 16, 20 and 24 elements will be calculated using equation (3.7). Besides calculation, the gain pattern of these numbers of elements at different angles will also be simulated using MATLAB software to view the effects of element number on the overall antenna radiation pattern.

All through the calculation, $d=0.5\lambda$, $\theta_0 = 90^\circ$, $\theta_s = 0^\circ$ and $\pi = 3.142$ respectively.

From equation 3.7,

$|G(\theta)| = |E_a(\theta)| = \frac{1}{N} \left| \frac{\sin(N2\pi/\lambda(d \sin(\theta_0 - \theta_s)/2))}{\sin(2\pi/\lambda(d \sin \theta/2))} \right|^2$

For N=4

$G(\theta) = \frac{1}{4} \left| \frac{\sin(4 \times 2 \times 3.142/\lambda(0.5\lambda \times \sin 90/2))}{\sin(2 \times \pi/\lambda(0.5\lambda \times \sin 90/2))} \right|^2$

$G(\theta) = \frac{1}{4} \times \left[\frac{0.1095}{0.0274} \right]^2 = \frac{15.97}{4} = 3.99$

$G(\text{db}) = 10 \log(3.99) = 6\text{db}$

For N=8;

$G(\theta) = \frac{1}{8} \left| \frac{\sin(8 \times 2 \times 3.142/\lambda(0.5\lambda \times \sin 90/2))}{\sin(2 \times \pi/\lambda(0.5\lambda \times \sin 90/2))} \right|^2$

$G(\theta) = \frac{1}{8} \times \left[\frac{0.217}{0.027} \right]^2 = \frac{64.59}{8} = 8.074; G(\text{db}) = 10 \log(8.07) = 9.06\text{db}$

For N= 16

$G(\theta) = \frac{1}{16} \left| \frac{\sin(16 \times 2 \times 3.142/\lambda(0.5\lambda \times \sin 90/2))}{\sin(2 \times \pi/\lambda(0.5\lambda \times \sin 90/2))} \right|^2 = \frac{1}{16} \times \left[\frac{0.4247}{0.0274} \right]^2 = 15.01$

$G(\text{db}) = 10 \log(15.01) = 11.8\text{db}$

For N=20

$G(\theta) = \frac{1}{20} \left| \frac{\sin(20 \times 2 \times 3.142/\lambda(0.5\lambda \times \sin 90/2))}{\sin(2 \times \pi/\lambda(0.5\lambda \times \sin 90/2))} \right|^2$

$= \frac{1}{20} \times \left[\frac{0.5212}{0.0274} \right]^2; G(90) = 18.09; G(\text{db}) = 10 \log(18.09) = 12.6\text{db}$

For N=24

$G(\theta) = \frac{1}{24} \left| \frac{\sin(24 \times 2 \times 3.142/\lambda(0.5\lambda \times \sin 90/2))}{\sin(2 \times \pi/\lambda(0.5\lambda \times \sin 90/2))} \right|^2$

$= \frac{1}{24} \times \left[\frac{0.6115}{0.0274} \right]^2; G(90) = 24.90; G(\text{db}) = 10 \log(24.90) = 14\text{db}$

From the calculations above, it can be seen that the gain of the 4-element array isotropic antenna has been enhanced from 6db to 14db by adding more elements to the array. To explain this further, the radiation pattern of the same number of array elements are simulated in MATLAB to view the increase in gain pattern as the number of radiating elements is increased (fig 3.2, 3.3, 3.4, 3.5, 3.6).

The radiation pattern shows how far down its sidelobes (undesired direction) are from the gain at the peak of the mainlobe (desired direction). It will be seen that as the number of elements increase in the array, the sidelobe levels also increase. This indicates that, as the gain in the desired direction increased, the gain in the undesired direction also increased relatively. Because of this undesirable sidelobes, further improvement will be done on the normalized gain pattern by optimizing the current excitation function (while keeping constant the exponential function), that will control sidelobe levels in the far field of the array.

The normalized field pattern is

$$|E_a(\theta)| = \frac{1}{\sqrt{N}} \left| \frac{\sin(N2\pi/\lambda(d \sin \theta/2))}{\sin(2\pi/\lambda(d \sin \theta/2))} \right| \dots\dots\dots (3.8)$$

This pattern is very useful in analyzing array problems showing important radiation properties such as Half Power Beamwidth, Sidelobes and directivity, and will be used in the next step to generate the fields of the individual elements with respect to scan angle.

N=4, d=0.5λ

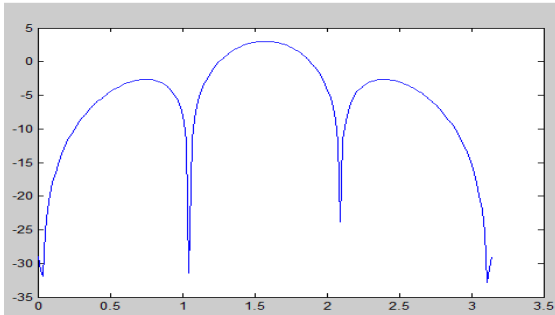


Fig 3.2 Gain as a function of scan angle (radians) for N=8, D=0.5λ

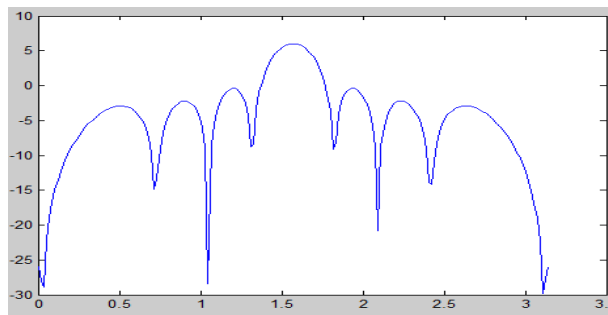


Fig 3.3 Gain as a function of scan angle

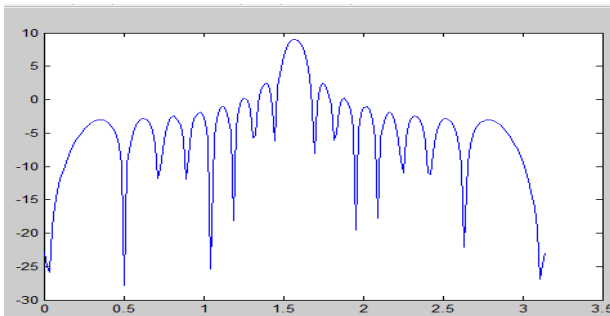


Fig 3.4 Gain as a function of scan angle (rad) for N=16, d=0.5λ

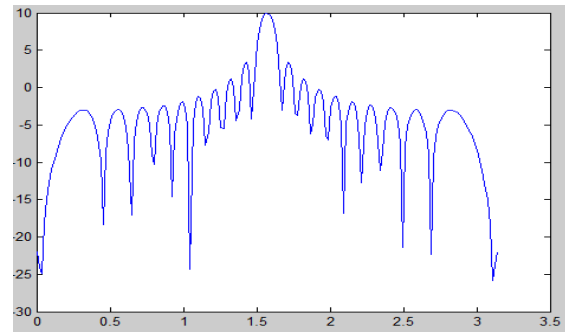


Fig 3.5 Gain as a function of scan angle

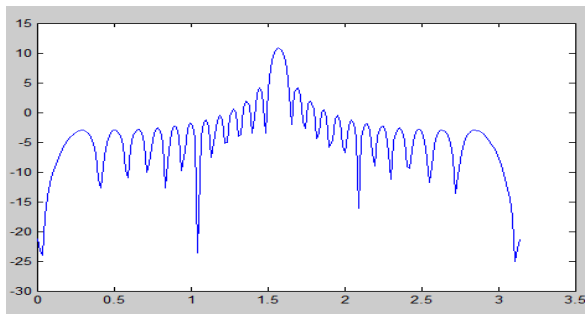


Fig 3.6 Gain as a function of scan angle (rad) for N=24, d=0.5λ

3.3.2 Design requirements for particle swamp optimization

In this stage of the work, a 24- element array is being optimized. For uniform excitation, the beamwidth of such an array is approximately 6° to 7° and sidelobe level about -18 dB. The design goal is that the phased

array will have SLL less than -20 dB and beamwidth of approximately 7°. These values are not chosen anyhow but are based on reference values. For a 24 element array, the lowest SLL level achievable by excitation optimization is about -20 dB. And by minimizing SLL, the beamwidth cannot be lowered more than 7°. However, a phased array for any arbitrary SLL and beamwidth can be designed using the same procedure used here by increasing or decreasing the number of array elements. So, the normalized desired pattern for a 24-element array is defined as:

$$FF_{\text{desired}}(\theta) = \begin{cases} 0\text{db}, & -3.5^\circ \leq \theta \leq 3.5^\circ \\ -20\text{db}, & \text{otherwise} \end{cases}$$

The radiation of the array for uniform excitation ($a_n = 1$) does not satisfy this design requirements. So, optimization is necessary. The fitness function (cost function) is defined as the sum of the squares of the excess far field magnitude above the desired pattern. So,

$$\text{fitness} = \begin{cases} \sum_{-90}^{90} [FF(\theta) - FF_{\text{desired}}]^2, & FF(\theta) > FF_{\text{desired}}(\theta) \\ 0, & \text{otherwise} \end{cases}$$

This type of fitness function definition is widely used for antenna array synthesis problems because it cuts off sidelobe levels above the desired envelope, while sidelobes below the specifications are neither penalized nor rewarded. The goal of the optimization process is to find the values of \mathbf{a}_n , so that the fitness function is minimized and the achieved radiation pattern matches closely with the desired pattern.

3.3.3 Particle Swarm Optimization Algorithm And Flowchart

The flowchart for PSO is given in Figure 3.7. The main steps of the PSO algorithm are given as follows:

Step 1: Initialize the particles X_i with initial random positions in search space, and the velocities of particles V_i in a given range randomly and define these as the best known positions (P_{best}) of each particle.

Step 2: Define the objective function f that needs to be optimized.

Step 3: For each particle calculate the distance to the optimal solution called fitness, and apply equation (3.9):

$$\text{If } f(x_i) < f(p_{\text{best}}) p_{\text{best}} = x_i \dots\dots\dots 3.9$$

Step 4: Select $\text{global}_{\text{best}}$ among the P_{best}

Step 5: If $f(\text{global}_{\text{best}})$ reaches to the optimal solution, terminate the algorithm. Otherwise; update the velocity V_i and the particles X_i according to given equations:

$$v_i = wv_i + c_1(p_{\text{best}} - x_i) + c_2(\text{global}_{\text{best}} - x_i) \dots\dots\dots 3.10$$

$$x_i = x_i + v_i \dots\dots\dots 3.11$$

Step 6: Go to Step 3, if stopping criteria are not satisfied

3.3.4 Modified Particle Swarm Optimization

In standard PSO, the velocity at each iteration step is calculated from:

$$v_n(t + 1) = wv_n(t) + C_1 r_1 \{x_{\text{pb},n} - x_n(t)\} + C_2 r_2 \{x_{\text{gb},n} - x_n(t)\} \dots (3.9)$$

Where r_1 and r_2 are two random numbers between 0 and 1, c_1 and c_2 are acceleration constants, w is the inertial weight, $x_{\text{pb},n}$ is the coordinate of the personal best position of the particle in n th dimension and $x_{\text{gb},n}$ is the coordinate of the global best position of the swarm in the n th dimension. The value of both acceleration constants c_1 and c_2 are taken to be 3, which are commonly used values. The two random variables are used to simulate the slight unpredictable component of natural swarms. The inertial weight, w , determines to what extent the particle remains along its original course and is not affected by the pull of personal best and global best. If t_{max} is the maximum number of iterations, then, w is expressed as:

$$W(t) = W_{\text{max}} - \frac{W_{\text{max}} - W_{\text{min}}}{t_{\text{max}}} t \dots\dots\dots (3.10)$$

The modified Gaussian linear equation is:

$$w(t) = w_{\max} - w_{\text{in}} \exp\left\{-\frac{y}{t_{\max}}\right\} + w_{\min} \dots \dots \dots (3.11)$$

Where, y is a constant whose value is taken to be 1.2. The function has the same initial and final values as the linear function, but it is characterized by a sharper rate of decrease. A small value of w encourages local exploitation whereas a larger value of w encourages global exploration. So, it is expected that the sharper fall of w will increase the rate of convergence without sufficiently reducing global search.

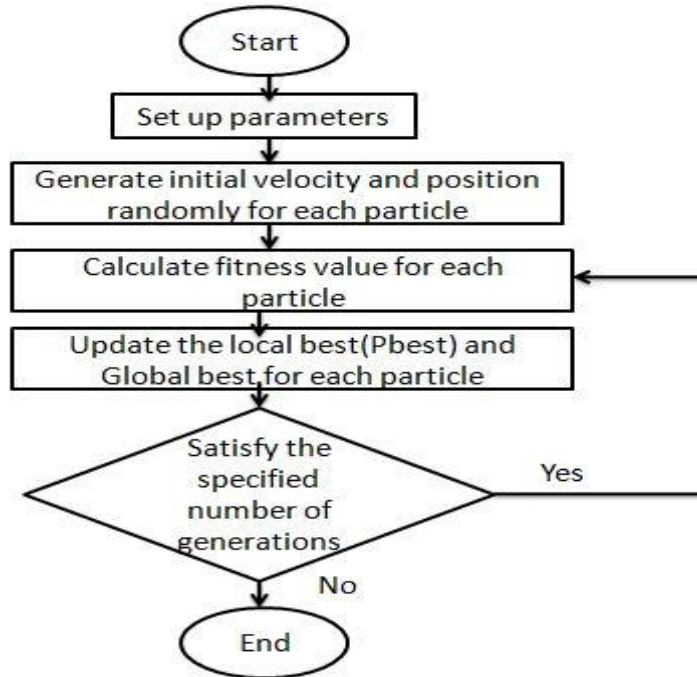


Fig 3.7 Flowchart of Particle Swarm Optimization

Using a simple linear relationship between the variables, the velocity update equation can be modified. This modified equation can be expressed as:

$$v_n(t + 1) = C_1 r_1 \{x_{pb,n} - x_n(t)\} + C_2 r_2 \{x_{gb,n} - x_n(t)\} \dots \dots \dots (3.13)$$

The modified PSO used here consists of this modified velocity update equation along with modified inertial weight variation function given by (3.11)

The optimization problem is modeled into minimum-maximum problem

IV. Results

4.1 Enhanced Pattern With Respect To Optimized Current Excitation

The results for the main lobe and the first sidelobe peaks of the normalized radiation pattern for 4, 8, 16, 20, and 24 isotropic elements with uniform current excitation are presented in table 4.1. The results for the optimized current excitations are presented in the Table 4.2, Table 4.3, Table 4.4, table 4.5 and table 4.6 for 4, 8, 16, 20 and 24 elements of the antenna array respectively. For each array, to show that the modified PSO has suppressed the sidelobe levels much more than the standard PSO, sidelobe levels are given at the end of the table. The excitation obtained through the algorithms are substituted for I in eqn 3.2 and used in the calculation of the field pattern for each array. The electric fields for 24 elements are presented in tables 4.7, 4.8, 4.9 and 4.10. **Ed** are the normalized electric fields of 24 elements with uniform currents, **Ed0** are the logarithmic electric fields elements with uniform currents (I=1), **Ed1** are the electric fields with optimized currents and **Ed2** are the electric fields with Modified optimized current amplitudes respectively. The radiation patterns for each set of elements are shown in the figures- fig4.1, Fig. 4.2, Fig. 4.3, fig. 4.4, and fig.4.5(a, b) respectively. Fig 4.6 is plotted from table 4.6. These optimized plots show the smooth reduction in the side lobe level in each case and meet the objective function of the algorithm of -20db.

Table 4.1 Gain and SLL of 4, 8, 16, 20 and 24 element with 4 elements

Number of elements	4	8	16	20	24
Gain	4.79	7.79	9.56	9.999	10.33
Sidelobe level	-2	-1	2.5	2.6	4.9

Table 4.2 synthesized currents

Element excitation	Uniform excitation	Standard Particle Swarm Optimization	Modified Particle Swarm Optimization
a_1	1	0.9792	1.0000
a_2	1	0.8975	0.9216
SLL	-15db	-100db	-100db
HPBW	40°	90°	90°

Table 4.3 synthesized currents with 8 elements

Element excitation	Uniform excitation	Standard Particle Swarm Optimization	Modified Particle Swarm Optimization
a_1	1	0.7077	0.7843
a_2	1	0.5390	0.6000
a_3	1	0.3805	0.4078
a_4	1	0.2601	0.2471
SLL	-18db	-20db	-23db
HPBW	15°	35°	30°

Table 4.4 synthesized currents with 16 elements

Element excitation	Uniform excitation	Standard Particle Swarm Optimization	Modified Particle Swarm Optimization
a_1	1	0.1452	0.1255
a_2	1	0.9228	0.0588
a_3	1	0.9323	0.9792
a_4	1	0.8646	0.8965
a_5	1	0.6184	0.7076
a_6	1	0.4226	0.3816
a_7	1	0.2636	0.2551
a_8	1	0.2636	0.2551
SLL	-15db	-21db	-24db
HPBW	10°	30°	25°

Table 4.5: Synthesized currents with 20 elements

Element excitation	Uniform excitation	Standard Particle Swarm Optimization	Modified Particle Swarm Optimization
a_1	1	0.9493	0.9098
a_2	1	0.9386	0.8667
a_3	1	0.8671	0.7608
a_4	1	0.8177	0.6667
a_5	1	0.6832	0.5333
a_6	1	0.6334	0.5132
a_7	1	0.5094	0.4431
a_8	1	0.3933	0.3020
a_9	1	0.3021	0.2196
a_{10}	1	0.2997	0.1725
SLL	-15db	-22db	-26db
HPBW	9°	15°	18°

Table 4.6: synthesized currents with 24 elements

Element excitation	Uniform excitation	SPSO	MPSO
a_1	1	0.0000	0.0000
a_2	1	0.1362	0.0311
a_3	1	0.2698	0.0655
a_4	1	0.3984	0.0982
a_5	1	0.5196	0.1313
a_6	1	0.6311	0.1539
a_7	1	0.7107	0.1967
a_8	1	0.8170	0.2284
a_9	1	0.8848	0.2643
a_{10}	1	0.9448	0.2953
a_{11}	1	0.9724	0.3964
a_{12}	1	0.9999	0.3811
SLL	-15db	-21db	-25db
HPBW	6°	15°	18°

Table 4.7 Generated Electric fields (ed)

FIELDS FOR UNIFORMLY EXCITATION CURRENTS (NORMALIZED)						
0.0000	0.0000	0.0000	0.0000	0.0000	0.0001	0.0001
0.0001	0.0002	0.0002	0.0002	0.0003	0.0003	0.0004
0.0005	0.0005	0.0006	0.0007	0.0008	0.0009	0.0010
0.0011	0.0012	0.0013	0.0014	0.0015	0.0016	0.0017
0.0019	0.0020	0.0022	0.0023	0.0024	0.0026	0.0028
0.0029	0.0031	0.0033	0.0034	0.0036	0.0038	0.0040
0.0042	0.0044	0.0046	0.0048	0.0050	0.0053	0.0055

Table 4.8: Generated Electric fields (ED0)

Fields For Uniformly Excitation Currents (Logarithmic)									
-324.2604	-112.4231	-100.3819	-93.3383	-88.3407	-84.4644	-81.2971	-78.6193	-76.2997	-74.2536
-72.4234	-70.7677	-69.2563	-67.8659	-66.5786	-65.3802	-64.2592	-63.2062	-62.2134	-61.2744
-60.3835	-59.5362	-58.7284	-57.9565	-57.2175	-56.5087	-55.8278	-55.1727	-54.5414	-53.9324
-53.3441	-52.7751	-52.2243	-51.6906	-51.1728	-50.6702	-50.1818	-49.7070	-49.2448	-48.7949
-48.3564	-47.9289	-47.5118	-47.1047	-46.7071	-46.3185	-45.9387	-45.5672	-45.2037	

Table 4.9 generated electric fields (ed1)

fields for non-uniformly excitation currents				
-322.4763	-133.2510	-121.2098	-114.1661	-109.1686
-105.2922	-102.1250	-99.4472	-97.1275	-95.0815
-93.2512	-91.5956	-90.0841	-88.6937	-87.4064
-86.2080	-85.0870	-84.0340	-83.0412	-82.1022
-81.2113	-80.3640	-79.5561	-78.7842	-78.0452
-77.3364	-76.6554	-76.0002	-75.3689	-74.7598
-74.1715	-73.6024	-73.0516	-72.5177	-71.9999
-71.4972	-71.0087	-70.5337	-70.0715	-69.6213
-69.1827	-68.755	-68.3378	-67.9305	-67.5327
-67.1439	-66.7639	-66.3922	-66.0284	

Table 4.10 Generated Electric fields (ED2)

Fields For Non-Uniformly Excitation Currents				
-326.8780	-131.7858	-119.7446	-112.7010	-107.7035
-103.8271	-100.6599	-97.9820	-95.6624	-93.6163
-91.7861	-90.1305	-88.6190	-87.2286	-85.9413
-84.7429	-83.6219	-82.5689	-81.5761	-80.6370
-79.7462	-78.8989	-78.0910	-77.3191	-76.5801
-75.8713	-75.1904	-74.5352	-73.9039	-73.2948
-72.7065	-72.1375	-71.5866	-71.0528	-70.5350
-70.0323	-69.5439	-69.0689	-68.6067	-68.1566
-67.7180	-67.2904			

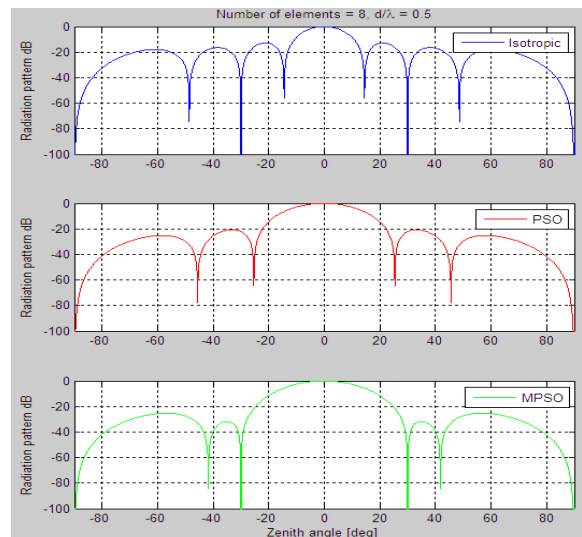
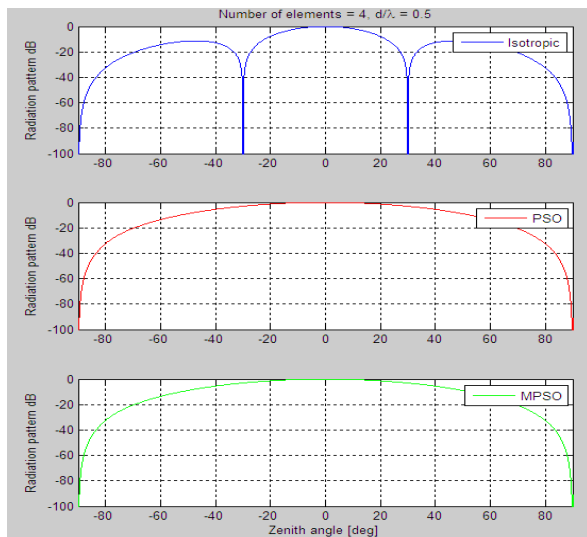


Fig 4.1: radiation pattern of a 4-element array scanned at broadside **Fig 4.2** radiation pattern of an 8-element array scanned at broadside

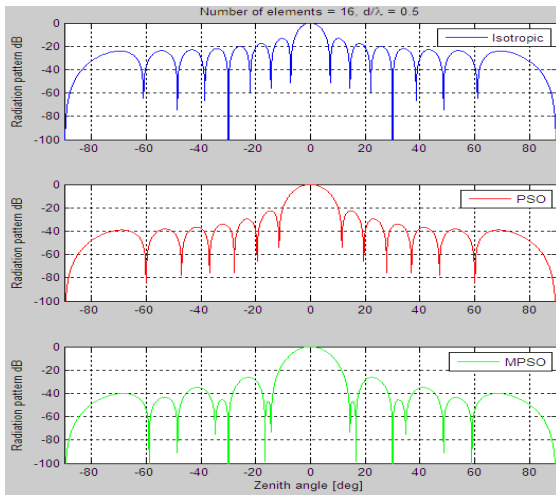


Fig 4.3 radiation pattern of a 16-element array scanned at broadside

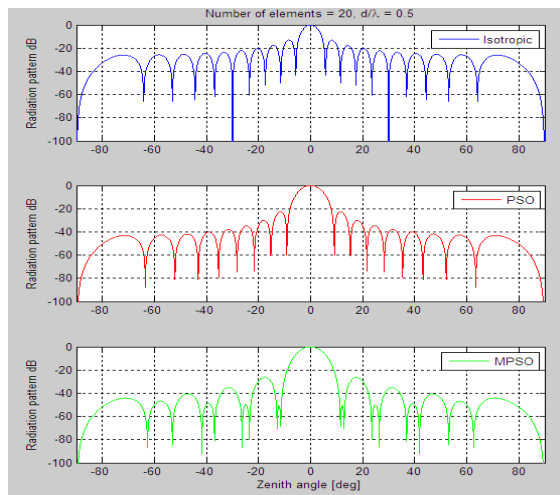
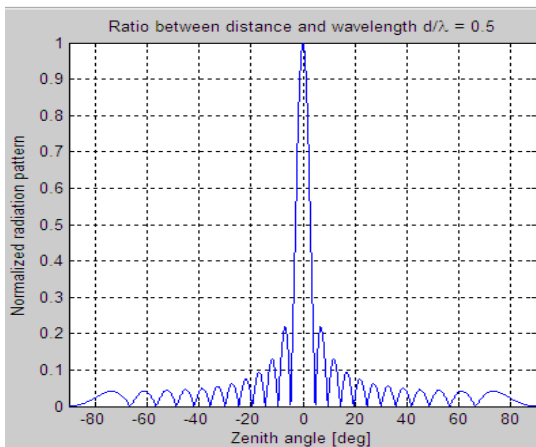


Fig 4.4 radiation pattern of a 20-element array scanned at broadside



4.5(a) Normalized radiation pattern of a 24 element linear broadside array

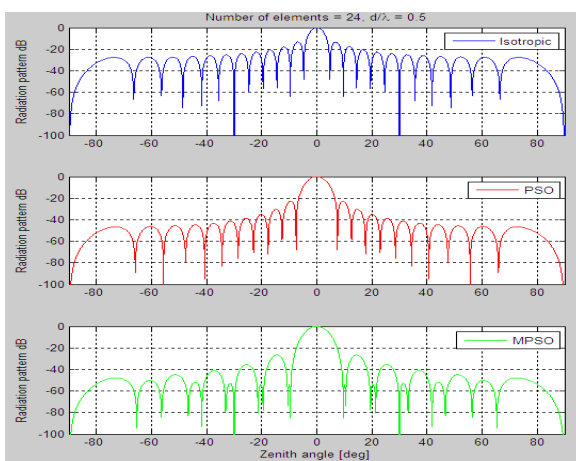
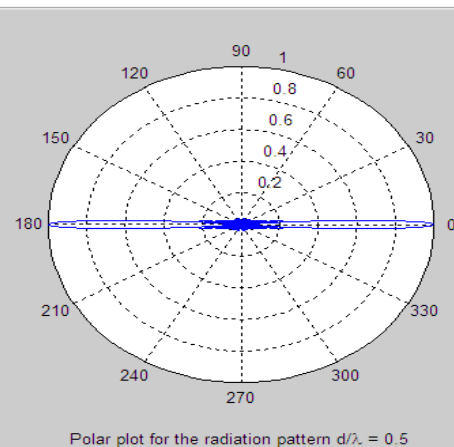


Fig 4.5(b) Logarithmic pattern of a 24-element array scanned at broadside

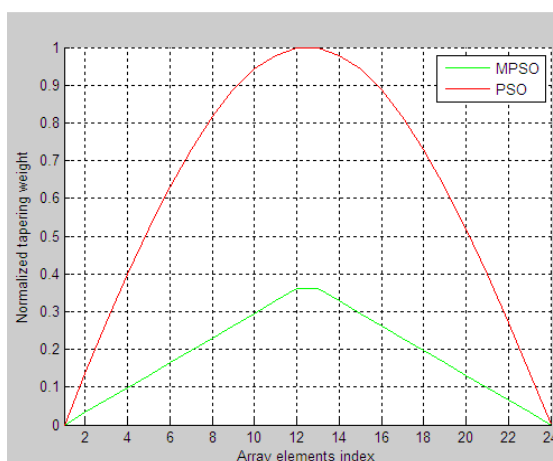


Fig 4.6 Normalized weight against array elements for PSO and MPSO

V. Conclusion

In this paper, the sidelobe level of 4, 8, 16, 20, and 24 isotropic elements have been suppressed using Particle Swarm Optimization. The Modified Particle Swamp Optimization produces better results than the Standard Particle Swamp Optimization. The side lobe level decreased up to -25 dB down the main lobe which represents the high reduction in the side-lobe level which is very much desirable to avoid radio frequency interference and sidelobe clutters in wireless communications. The side lobe reduction is more useful in GSM

(Global System for Mobile communication), RADAR (Radio Detection And Ranging), SONAR (Sound Navigation And Ranging) and image mapping; especially in RADAR application where high side lobes can detect false target and lead to unintended signal jamming.

References

- [1]. Balanis, C. A, Antenna Theory: Analysis and Design, 3rd ed., Hoboken: John Wiley, 2005, pp. 300-304.
- [2]. Basker S, Alphones A, Suganthan P. N, Genetic Algorithm based design of a reconfigurable antenna array with discrete phase shifters, Wiley Online library, 2005.
- [3]. Dahab.A ,1994: A new technique for linear antenna array processing for reduced sidelobes using neural networks,
- [4]. Drabowitch S, Papiernik A, Griffiths H, Encinas J, & Bradford L. Smith, Modern Antennas, Chapman & Hall, London, pp. 400-402, 1998.
- [5]. Haupt R. L, "Directional Antenna System Having Sidelobe Suppression", Us Patent 4, pp571- 594 Feb 18, 1986.
- [6]. Pallavi Joshi, Optimization of linear antenna array using genetic algorithm for reduction in side lobe levels and to improve directivity, international journal of latest trends in engineering and technology, vol 2, may 2013.
- [7]. P-N Designs Inc. (2008, June). Phase Shifters. microwaves101.com [Online]. Available: <http://www.microwaves101.com/encyclopedia/phaseshifters.cfm>
- [8]. Rahmat-sammii, Y, Colburn, J. S Patch antennas on externally perforated high dielectric constant substrates, 1999, Los Angeles.
- [9]. Safaai-Jazi A, A new formulation for the design of Chebyshev arrays, IEEE transactions on 42(3), 439-443, 1994

Authors' Biography

Biebuma Joel Jeremiah holds a B.Eng & M.Sc (S.C.T, Sussex, England) in Electronic & Communication Engineering, & Ph.D (S.C.U, California, U.S.A) in Telecommunication Engineering . He is a member, Nigeria Association for Teachers of Technology (MNATT), Member Institute of Electronics and Electrical Engineers (MIEEE) and Member, Nigeria Society of Engineers. His research interest is in Electronics, Telecommunication, Antennas, Microwaves etc. He is a prolific writer with numerous technical papers and engineering text books. He is currently a Senior Lecturer and Ag. HOD, Department of Electronic and Computer Engineering, University of Port Harcourt, Port Harcourt, Nigeria. He is happily married with Children.



Bourdillon .O. Omijeh holds a B.Eng degree in Electrical/Electronic Engineering, M.Eng and Ph.D .Degrees in Electronics/Telecommunications Engineering from the University of Port Harcourt & Ambrose Alli University (A.A.U), Ekpoma respectively. His research areas include: Artificial Intelligence, Robotics, Embedded Systems Design, Modeling and Simulation of Dynamic systems, Intelligent Metering Systems, Automated Controls, Telecommunications and ICT. He has over thirty (30) technical papers & publications in reputable International learned Journals and also, has developed over ten (10) application Software. He is a member, Institute of Electronics and Electrical Engineers (MIEEE), Member, Nigeria Society of Engineers; and also, a Registered Engineer (COREN). He is currently a Senior Lecturer & pioneer HOD, Department of Electronic and Computer Engineering, University of Port Harcourt, Nigeria; and also, a consultant to companies & Institutions. He is happily married with Children. E-mail: bourdillon.omijeh@uniport.edu.ng.



Jackson Eno Linus holds a B.Eng Degree in Electrical/Electronic Engineering from the University of Uyo, Uyo. Her research areas includes: voltage regulators, fibre optics, automated controls and antennas. She is currently carrying out a research work on enhancing the gain of phased array antenna in her Masters' Degree Programme at Department of Electronic & Computer Engineering, University of Port Harcourt, Nigeria.